CRYSTAL GROWTH & DESIGN

Article

pubs.acs.org/crystal

A $CdSO_4$-Type 3D Metal–Organic Framework Showing Coordination Dynamics on Cu^{2+} Axial Sites: Vapochromic Response and Guest Sorption Selectivity

Guo-Bi Li, Lei Li, Jun-Min Liu,* Tao Yang, and Cheng-Yong Su*

KLGHEI of Environment and Energy Chemistry, MOE Laboratory of Bioinorganic and Synthetic Chemistry, State Key Laboratory of Optoelectronic Materials and Technologies, School of Chemistry and Chemical Engineering, Sun Yat-Sen University, Guangzhou, 510275, China

Supporting Information

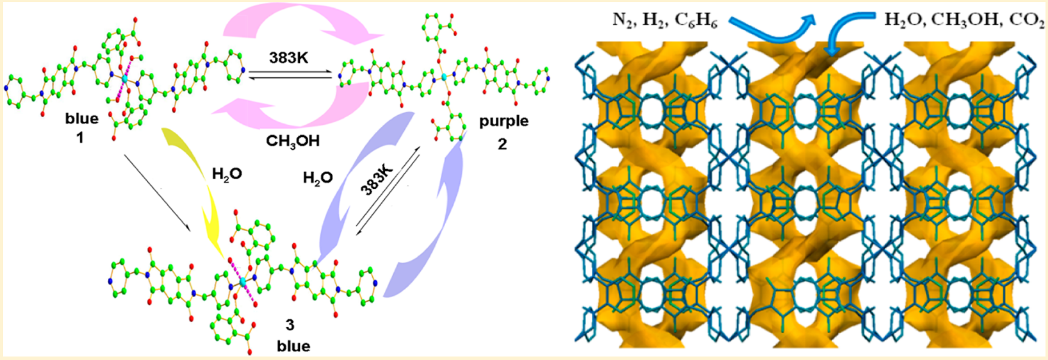

ABSTRACT: A unique 2-fold interpenetrated $CdSO_4$ coordination network of the formula $\{[Cu_2(4\text{-pmpmd})_2(CH_3OH)_4(opd)_2]\cdot 2H_2O\}_n$ [4-pmpmd = *N,N'*-bis(4-pyridylmethyl)phenyldiimide; opd = *o*-phthalic acid] has been synthesized and characterized by IR spectra, thermogravimetric (TG) analyses, elemental analyses, and single crystal and powder X-ray diffraction methods. The metal–organic framework (MOF) exhibits reversible dehydration and rehydration in a single-crystal-to-single-crystal (SC–SC) process. Moreover, the dehydrated material, having coordinatively unsaturated Cu^{2+} sites, can encapsulate CH_3OH molecules with a color change, again in a reversible SC–SC fashion, and shows selective adsorption of CO_2 over N_2 and H_2. This feature of obvious color variation induced by the presence of small hydroxylic molecules is highly promising for detecting hydroxylic molecules through a simple sensing mechanism. In addition, the MOF selectively interacts with hydroxylic guests and shows sorption selectivity for water, methanol, ethanol, and *n*-propanol over benzene guests. Notably, this compound shows complete selectivity in adsorption for *n*-propanol over 2-propanol owing to the effect of shape exclusion.

■ INTRODUCTION

Metal–organic frameworks (MOFs) have attracted great attention due to their diverse architectures and potential applications in adsorption separations, sensing, gas storage, and catalysis.[1] MOFs with switchable or tunable properties are of great current interest for their highly sensitive response to small molecules and potential applications in chemical sensors.[2,3] Flexible frameworks are very sensitive to the guest molecules and undergo remarkable variations in structures and physical properties upon removal and uptake of guest molecules by the shrinkage/expansion or sliding motions. The available free volume in channels of the flexible frameworks is usually occupied by solvent and/or guest molecules, which must be exchanged or removed for exploiting the porous features. But in most cases, the single crystallinity of MOFs is not maintained after guest molecules are exchanged or removed or some other physical stimuli occur, since the simultaneous shrinking or expansion of the overall framework may lead to its breakdown. Therefore, the single-crystal-to-single-crystal (SC–SC) transformation is eagerly desirous, since it allows direct visualization of how the crystal structure is changed during the transformation process. These direct insights further the understanding of the subtle interaction between the guest molecules and the framework, which may opens new ways to study gas storage, separation, sensing, and catalysis. So far, the exploration of selective adsorption and sensing for small molecules, such as water and methanol, via SC–SC transformations is rare.

Some intriguing examples of well-designed porous structures with remarkable sensing selectivity have been reported, and most of the complexes reported up to now were dependent on the special pore sizes or open metal sites.[4] To achieve these targets, two types of strategies are used: incorporation of coordinatively unsaturated metal centers and introduction of

Received: November 30, 2012
Revised: March 9, 2013

dx.doi.org/10.1021/cg3017563 | *Cryst. Growth Des.* XXXX, XXX, XXX–XXX

organic groups to provide guest-accessible functional organic sites.[5] However, the chance of finding a MOF that contains coordinatively unsaturated metal centers and yet exhibits permanent porosity is rare, as only a few MOFs are stable upon thermal liberation of volatile coordinated ligands.[6] However, it is of great current interest due to their highly sensitive response to small molecules and potential applications in chemical sensors.[7] In particular, coordinatively unsaturated metal complexes could display an absorption in the visible region of the spectrum that can be tuned by binding of guest species to the metal center, thus offering the possibility of a selective colorimetric detection of guest molecules even by the naked eye.[8] On the other hand, successful immobilization of guest-accessible functional organic sites onto the MOF pore surface is still difficult because organic groups tend to coordinate metal ions in a self-assembly process to give a framework in which functional organic sites are completely blocked.[9] Therefore, introducing a functional part into open-framework materials that tunes framework flexibility and structural dynamism is an important challenge for crystal engineers and in the fabrication of new materials.[10]

Here we report the structure and properties of a 2-fold interpenetrating $CdSO_4$ network topology **1**, synthesized from a bidentate ligand with flexible arms ($-CH_2-$) and a second building unit with functional groups ($-C{=}O$), which shows a dynamic behavior, directly visualized by SC−SC transformations. The process involves an unusual change in the coordination number of the copper center owing to the reversible removal of methanol molecules coordinated to Cu^{2+}. The desolvated phase **2** containing coordinatively unsaturated metal centers shows a highly selective sensing and sorption behavior toward some specific adsorbates, and the selectivity mainly arises from the interactions between the adsorbates and the coordinatively unsaturated Cu^{2+} metal sites or/and hydroxyl groups on the surface of the adsorbent.

■ EXPERIMENTAL SECTION

Physical Methods. All materials were reagent grade, obtained from commercial sources, and used without further purification. Solvents were dried by standard procedures. The ligand was prepared according to previous literature methods.[11] Elemental analyses (C, H, N) were carried out with a Perkin-Elmer 240C elemental analyzer. FT-IR spectra were recorded from KBr pellets in the range of 4000−400 cm^{-1} on a VECTOR 22 spectrometer. The powder X-ray diffraction (PRXD) was recorded on a Bruker D8 ADVANCE diffractometer (Cu Kα, 1.5418 Å) at 40 kV and 40 mA. Thermal analyses were performed on a TGA V5.1A Dupont 2100 instrument from room temperature to 800 °C with a heating rate of 10 °C min^{-1} in the air, and the data are consistent with the structures. The adsorption isotherms of CO_2 (at 195 K) and N_2 and H_2 (at 77 K) were measured by using BELmax 00027 adsorption equipment (BEL Japan). The methanol (298 K), alcohol (298 K), and toluene (298 K) vapor were measured with a BELSORP-max automatic volumetric sorption apparatus. An exactly measured amount of the sample was introduced into the gas sorption instrument after the sample was predesolvated in a Schlenk tube at 120 °C under vacuum for 24 h. The adsorbate was placed into the sample tube, and then the change of the pressure was monitored and the degree of adsorption was determined by the decrease of the pressure at the equilibrium state. The sorption properties were analyzed using Autosorb 1 for Windows 1.24 software.

Preparation of $\{[Cu_2(4\text{-pmpmd})_2(CH_3OH)_4(opd)_2]\cdot 2H_2O\}_n$, 1. A mixture of $CuCl_2\cdot 4H_2O$ (21 mg, 0.1 mmol), 2,6-bis(4-pyridinylmethyl)benzo[1,2-*c*:4,5-*c*′]dipyrrole-1,3,5,7(2*H*,6*H*)-tetrone (4-pmpmd) (40 mg, 0.1 mmol), disodium phthalate (21 mg, 0.1 mmol), CH_3OH (6.0 mL), and $CHCl_3$ (12.0 mL) was heated in a 20 mL Teflon-lined autoclave for 7 days at 110 °C, cooled to 80 °C, maintained at this temperature for 1 day, and then allowed to cool slowly to room temperature. Blue crystals were obtained together with a large amount of blue crystalline solids. The yield is estimated at about 35% on the basis of the original ligand. IR (KBr, cm^{-1}): 3477s, 3125w, 3032w, 2956w, 2113s, 1774s, 1715s, 1621s, 1430m, 1393s, 1368s, 1336m, 1314w, 1262m, 1180w, 1128m, 1072w, 1034m, 964w, 939m, 789s, 733s, 645m, 598w, 485m. Anal. Calcd for $C_{64}H_{56}O_{22}N_8Cu_2$: C, 54.28; H, 3.99; N, 7.91. Found: C, 54.37; H, 4.06; N, 7.95. Phase purity was verified by powder XRD.

Hydrated $[Cu(4\text{-pmpmd})(H_2O)_2(opd)\cdot 2H_2O]_n$, 3. . The single crystal **1** was heated at 110 °C under an air atmosphere for 2 h and exposed to air for several days, resulting in complete rehydration and formation of hydrated crystal **3**. IR (KBr, cm^{-1}): 3430s, 1773w, 1716s, 1620m, 1565m, 1427w, 1393s, 1364m, 1157w, 1121w, 1090w, 942m, 754w, 727m, 631w, 587w. Anal. Calcd for $C_{30}H_{26}O_{12}N_4Cu$: C, 51.62; H, 3.75; N, 8.03. Found: C, 51.35; H, 4.06; N, 7.97.

X-ray Data Collection and Structure Refinement. The diffraction data were collected on a Oxford Gemini S Ultra diffractometer equipped with Cu Kα radiation (λ = 1.541 78 Å) for complexes **1**, **1′**, **2**, **3**, and **3′** by using φ and ω scans. Analytical adsorption corrections were applied for complexes **2** and **3**. Multiscan adsorption corrections were applied for all others. The structures were solved by the direct methods (SHELXS) and refined by the full matrix least-squares method against F_o^2 using the SHELXTL software.[12] The coordinates of the non-hydrogen atoms were refined anisotropically. Most of hydrogen atoms were introduced in calculated positions and refined with fixed geometry with respect to their carrier atoms, and the hydrogen atoms of water have been not added. Details of the crystal parameters, data collections, and refinement for the five complexes **1**, **1′**, **2**, **3**, and **3′** are summarized in Tables 1 and 2. Further details are provided in the Supporting Information. Crystallographic data for the structures reported in this paper have been deposited with the Cambridge Crystallographic Data Centre as supplementary publication no. CCDC 858869, 858870, 858871, 858872, 858873 for the five new compounds **1**, **1′**, **2**, **3**, and **3′**, respectively.

Table 1. Crystallographic Data for 1−3[a]

	1	2	3
empirical formula	C_{64} H_{58} Cu_2 N_8 O_{23}	C_{30} H_{18} Cu N_4 O_8	C_{30} H_{18} Cu N_4 O_{13}
formula weight	1434.26	626.02	706.02
space group	*Ibca*	*Ibca*	*Ibca*
crystal system	orthorhombic	orthorhombic	orthorhombic
a (Å)	15.2841(10)	14.6232(10)	14.9179(19)
b (Å)	16.7279(10)	16.9144(10)	16.766(2)
c (Å)	27.5547(15)	27.9419(18)	27.650(3)
α (deg)	90	90	90
β (deg)	90	90	90
γ (deg)	90	90	90
V ($Å^3$)	7044.9(7)	6911.2(8)	6915.6(14)
Z	4	8	8
ρ_{calcd} (g cm^{-3})	1.352	1.203	1.356
T (K)	150(2)	383(2)	150(2)
μ (mm^{-1})	1.426	1.308	1.483
GOF	1.087	1.013	1.044
R_{int}	0.0634	0.0620	0.0886
R_1 [$I > 2\sigma(I)$]	0.0764	0.0524	0.0841
wR_2 (all data)	0.1999	0.1447	0.2337

[a] Crystallographic data for the structures reported in this table have been deposited with the Cambridge Crystallographic Data Centre as supplementary publication no. CCDC 858869, 858871, and 858872. Copies of the data can be obtained free of charge from www.ccdc.cam.ac.uk/conts/retrieving.html.

Table 2. Crystallographic Data for 1′ and 3′ Measured at Different Temperature[a]

	1′	3′
empirical formula	$C_{64}H_{58}Cu_2N_8O_{23}$	$C_{30}H_{18}CuN_4O_9$
formula weight	1434.26	642.02
space group	*Ibca*	*Ibca*
crystal system	orthorhombic	orthorhombic
a (Å)	15.3107(15)	14.7932(8)
b (Å)	16.7284(19)	16.7885(7)
c (Å)	27.412(5)	27.7725(16)
α (deg)	90	90
β (deg)	90	90
γ (deg)	90	90
V (Å^3)	7020.8(16)	6897.5(6)
Z	4	8
ρ_{calcd} (g cm^{-3})	1.357	1.237
T (K)	150(2)	150(2)
μ (mm^{-1})	1.430	1.346
GOF	1.081	1.002
R_{int}	0.0415	0.0363
R_1 [$I > 2\sigma(I)$]	0.0668	0.0463
wR_2 (all data)	0.1911	0.1460

[a] Crystallographic data for the structures reported in this table have been deposited with the Cambridge Crystallographic Data Centre as supplementary publication no. CCDC 858870 and 858873. Copies of the data can be obtained free of charge from www.ccdc.cam.ac.uk/conts/retrieving.html.

■ RESULTS AND DISCUSSION

Preparation and X-ray Structure of 1. Blue crystals of **1** [{[Cu_2(4-pmpmd)$_2$(CH_3OH)$_4$(opd)$_2$]·$2H_2O$}$_n$ (4-pmpmd = *N*,*N*′-bis(4-pyridylmethyl)phenyldiimide; opd = *o*-phthalic acid)] were obtained from 4-pmpmd, $CuCl_2·4H_2O$, and disodium phthalate in a mixture of methanol and chloroform by solvothermal synthesis. The crystal structure was determined using X-ray crystallography, and the building unit with the atom-labeling scheme is shown in Figure 1a. In **1**, each octahedral Cu^{2+} ion sits in a special position attached to two nitrogen atoms (N1 and N1′) via the two 4-pmpmd ligands, two oxygen atoms (O5 and O5′) via the two opd ligands, and two apical oxygen atoms (O3 and O3′) via methanol molecules. The distances of Cu−N and Cu−O bond coordinated with two ligands are 2.024(4) and 1.973(3) Å, respectively. However, the other Cu−O bond length is 2.453 Å, implying that the interaction of Cu^{2+} ion and methanol is a weak coordination. Cu^{2+} ions are bridged by pyridyl groups in N1−Cu−N1′ (180°) angle to form a 1D zigzag chain that extends along the *b*- and *c*-directions, and the intrachain Cu···Cu distance is 17.837 Å (Figure 1b). The opd ligand, acting as a bisconnector, links Cu to form the 1D zigzag chain complexes running along the *a*-axis with the Cu···Cu distance of 7.642 Å (Figure 1c). These three 1D chains are interconnected with each other in the crystal packing, and this continuous network forms the 2-fold interpenetrating 3D $CdSO_4$ net structure (Figure 1d). Each opd ligand bridges two Cu^{2+} anions, every 4-pmpmd ligand connects two Cu^{2+} anions, one of the 4-pmpmd ligands points down, and one of 4-pmpmd ligands points up, to form a tetragonal cage with a volume of 1018 Å^3 (Figure 1e). The resultant 3D framework contains 1D circular channels (6.48 Å, V_{void} = 23.4% of the total crystal volume) along the crystallographic *a*-axis, occupied by water guest molecules, which are H-bonded with the carbonyl groups of the ligand and the coordinated methanol molecules.

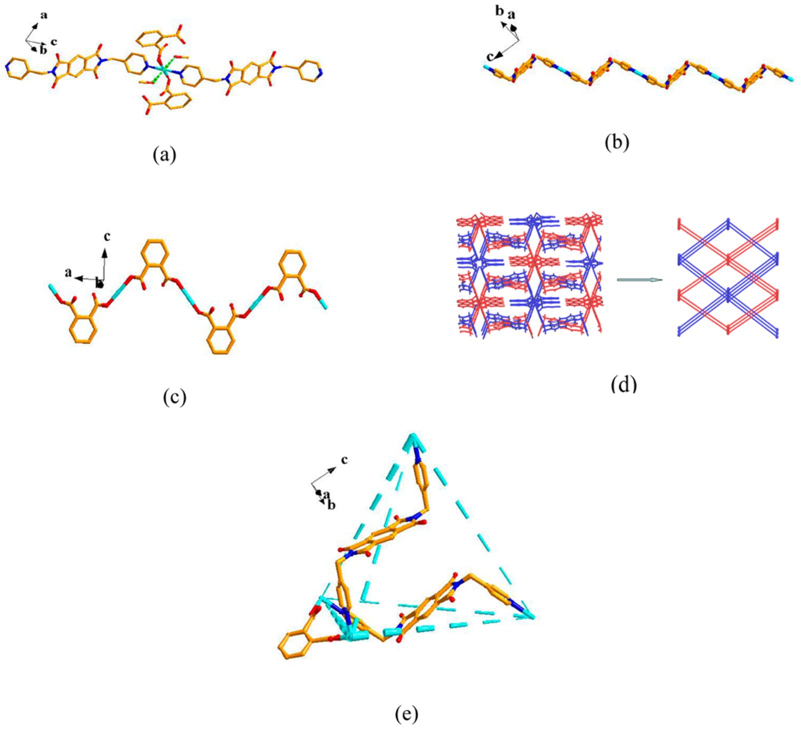

Figure 1. (a) The coordination environments of Cu^{2+} ion in **1**. (b) The 1D zigzag chain formed by Cu^{2+} ions bridging 4-pmpmd ligands. (c) The 1D zigzag chain formed by Cu^{2+} ions bridging opd ligands. (d) The 2-fold interpenetrating 3D $CdSO_4$ net structure constructed by three interconnecting 1D chains. (e) The 3D framework containing 1D zigzag channels occupied by water molecules. Hydrogen atoms are omitted for clarity. Symmetry codes: (a) $0.5 - x, -y, 0.5 + z$; (b) $-x, 0.5 + y, 0.5 - z$; (c) $0.5 + x, 0.5 - y, -z$.

A Single-Crystal-to-Single-Crystal Transformation among 1, 2, and 3. Guest solvent molecules occupied in cavities or channels can often be removed without causing framework collapse and, furthermore, can sometimes also be reinserted.[13] To explore this possibility, blue single crystal **1** was heated and then analyzed. Temperature-dependent XRPD measurements of **1** were first carried out, the result of which shows that the framework is robust and is maintained even without any solvent molecules being present at 200 °C (Figure S1, Supporting Information). Subsequently, the desolvated crystal $[Cu(4\text{-pmpmd})(opd)]_n$ (**2**) was obtained by heating the single crystal **1** at 110 °C under an air atmosphere for a period of 2 h. The X-ray structure of **2** indicates that the porous structure with a 3D interpenetrating framework is retained after removal of the coordinated methanol and guest water molecules (Figure 2). Although the crystal system and space group remain unchanged, the 3D framework is significantly changed from that of **1** in that the copper center in **2** is now only four-coordinate and has changed from an octahedral (as in **1**) to a square planar coordination environment. This is accompanied by a sharp change in color from blue to violet (Figure 3). Moreover, a mismatch between the number of coordination sites occupied by methanol in **1** and the number of coordination sites required for complete coordination of ligands indicates that there are coordinatively unsaturated metal sites in **2**. Due to these open metal sites and permanent porosity, **2** is expected to be useful for attaining high gas take.

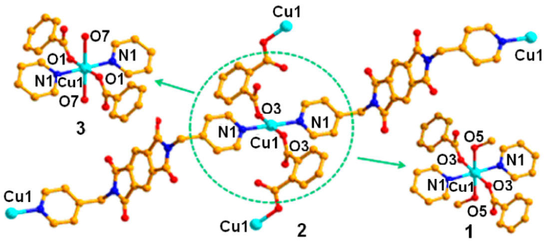

Figure 2. The coordination environments of Cu^{2+} ion in **1**−**3**.

Figure 3. The color changes of crystal **1** at different temperatures.

The single-crystal X-ray structure of violet **2** reveals that although the cross section of the 1D circular channel shrinks from 6.48 to 5.66 Å, the void space in **2**, which may be generated after removal of the coordinating methanol molecules, increases to 31.0% as opposed to 23.4% in **1** (Figure 4). It is noteworthy that the framework can easily make some adjustments with available free space to absorb some specific materials, due to the flexible $-CH_2-$ parts of the ligand. When a single crystal of **2** was immersed in methanol for a period of more than 1 d, the violet color of **2** returned to the blue color of the crystal **1**′. Single-crystal cell measurement reveals that **1**′ has reconstituted the original structure of **1**, that is, the dynamic structural transformation is reversible.

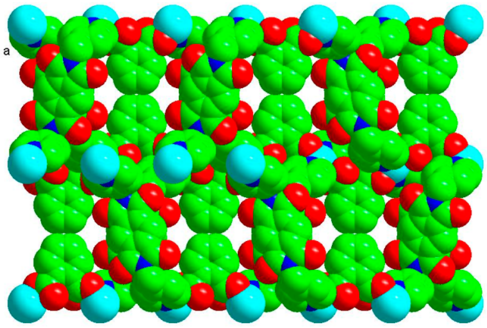

Figure 4. The 3D void framework of **2** upon removal of guest molecules.

Interestingly, brief immersion of single crystal **2** into water or exposure to air for several days results in complete rehydration and formation of hydrated crystal $[Cu(4\text{-pmpmd})(H_2O)_2(opd)\cdot 2H_2O\}]_n$ (**3**), including two coordinated water molecules and three guest water molecules. Thus, the rehydration process is accompanied by return of the original blue color. The single-crystal X-ray structure determination of **3** revealed that the crystal system and space group remain the same as those of **2**, but the copper center has re-form from a square planar (as in **2**) to an octahedral coordination environment, owing to the introduction of coordinated water molecules. It is worth mentioning that on rehydration the two closely packed interpenetrating networks undergo stress relax, which is due to the expansion of the channel size (5.72 Å) to provide a void space composing 31.3% of the total crystal volume. The TG profile of **3** also exhibits a stepwise release and shows that all the coordinated and uncoordinated water molecules are lost at 80 °C (calcd, 10.0%; found, 9.8%) (Figure S2, Supporting Information). Thus, heating **3** to 110 °C for **2** h completely reverses the structural change, and the original material **2** is reconstituted after the removal of all the water molecules. After determining the structure, the simulated powder X-ray diffraction (XRPD) was found to match that of as-synthesized compound **1**.

To investigate the dynamic structural transformation between **1** and **3**, single crystal **1** was immersed into water for several days and analyzed by single-crystal X-ray diffraction. Surprisingly, the methanol molecular coordinated to copper in **1** was completely replaced by water molecule, and crystal **3**′ was obtained, whose structure is the same as **3**. However, immersion of **3** into methanol heated to 75 °C for several days did not result in a structural change (Figure 5). This may be due to the fact that the binding of Cu^{2+} ion with water is stronger than with methanol.

Thermal Stability. The stepwise thermogravimetric curve of **1** indicates that the release of the guest water molecules and coordinated methanol molecules occurred at 77 °C to give the desolvated form, $[Cu(4\text{-pmpmd})(opd)]_n$ (**2**), which is stable up to 210 °C (calcd, 14.0%; found, 14.4%). Therefore, the desolvation can be accomplished by heating at the temperature range between 77 and 210 °C. On further heating, one 4-pmpmd molecule is lost at a temperature of 400 °C, and then the compound decomposes to form unidentified products (Figure S2a, Supporting Information). For **2**, the first step occurs in the range of 25−250 °C, corresponding to no escape

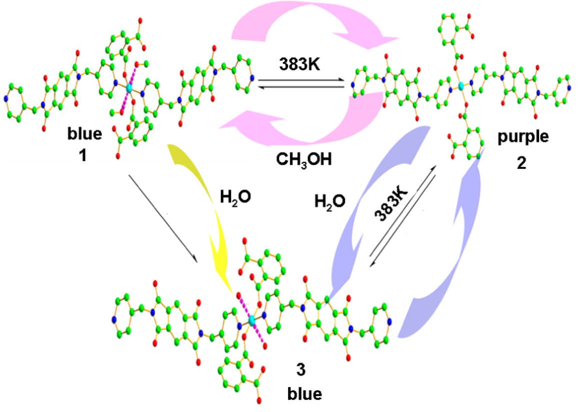

Figure 5. Reversible single-crystal-to-single-crystal transformations among **1**, **2**, and **3**.

of guest molecules, which proves **2** to be the void framework. The complete decomposition of the complex finishes at about 500 °C (Figure S2b, Supporting Information). The TG profile of **3** also exhibits a stepwise release and shows that all the coordinated and uncoordinated water molecules are lost at 80 °C (calcd, 10.0%; found, 9.8%) (Figure S2c, Supporting Information).

Selective Sensing of Small Hydroxylic Molecules by 2. Upon immersing the complex **2** into water or methanol for 30 min, it is interesting to find that **2** shows selective sensitivity to small hydroxylic molecules, with a visual color change from purple to blue, while other solvents such as ethanol, chloroform, acetone, benzene, THF, and DMF (**2** dissolves in DMSO) fail to induce a color change that could be discerned by eyes. The UV−vis spectra of blue **3**, which formed by immersing **2** in water, and purple **2** show a broad d−d absorption band at 670 and 530 nm, respectively (Figure S3, Supporting Information). Compared with the spectrum of purple **2**, there is about 140 nm red shift of the absorption band induced by water molecule coordination in the spectrum of **3**, which can be assigned as the LMCT transition and corresponds to the excitation wavelength. Therefore, **2** represents a structurally simple copper(II)-based optical sensor for small hydroxylic molecules whose response is determined by a shift of the metal-based d−d absorption upon binding of the methanol or water to the metal center, with a consequent complexation of the metal center from the ligand.[8,14] On the other hand, when the complex **2** is exposed to water or methanol vapor, its color also changes from purple to blue. This feature of obvious color variation induced by the presence of small hydroxylic molecules is highly promising for detecting small guest molecules through a simple sensing mechanism. The detection limits for water (100 ppm) and methanol vapor (150 ppm) of complex **2** have been determined by exposing **2** to water and methanol vapor with different concentrations, respectively. The exposure time is set as 5 min. The complex **2** also exhibits excellent recyclability on sensing. When purple **2** is exposed to water, its color turned to blue. After evacuation at 150 °C for 6 h, the purple color of **2** can be recovered, which can be used to detect water molecules again. The UV−vis spectra reveal that the color change from purple to blue between **2** and **3** is reversible (Figure S3, Supporting Information). In particular, the TGA studies indicate that the guest water molecules in the pores of **3** could be desorbed by heating it to 150 °C and readsorbed by exposing the material to the air upon cooling to room temperature. These procedures were repeated for several cycles to establish the reversibility of the process (Figure 6).

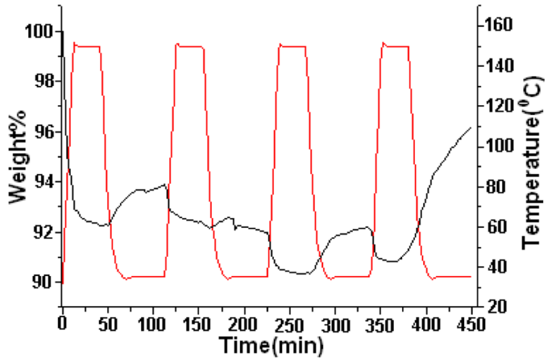

Figure 6. TGA measurements of cyclic water desorption and absorption processes for **3** were repeated. The variation of weight loss with time is shown as a black line. The variation of temperature with time is shown as a red line.

Sorption Properties of 2. To study the effect of structural transformation and verify the porosity of **2**, which contains coordinatively unsaturated Cu^{2+} ions, the gas sorption properties were measured for N_2 (kinetic diameter = 3.64 Å), H_2 (2.8 Å), and CO_2 (3.3 Å) gases. All adsorption isotherms of **2** show type I behavior, as expected for materials with micropores (~5 Å). (Figure 7a). Interestingly, **2** can absorb a significant amount of CO_2 at 1 atm and 77 K [84.6 cm^3 g^{-1} (STP)], exhibiting highly selective sorption of CO_2 over N_2 [12.4 cm^3 g^{-1} (STP)] and H_2 [4.4 cm^3 g^{-1} (STP)]. It was also observed that there is some sort of hysteresis between CO_2 sorption/desorption curves, which might originate from the strong interactions of CO_2 molecules with the host solid **2** and/or a dynamic structural transformation from desolvated to guest occupied structure. The different adsorption capabilities for gases can be ascribed to the existence of a larger quadrupolar moment for CO_2 (quadrupolar moment = 4.30×10^{26} esu cm^2) than N_2 (1.52×10^{26} esu cm^2) and H_2 (0.662×10^{26} esu cm^2), thereby providing stronger framework partial charge/quadrupole interactions for CO_2. We reasoned that the open metal sites in **2** also might enhance the selectivity. The capture and separation of carbon dioxide is important for the safe storage of carbon into deep geological formations, and this selectivity can be used for CO_2 separations from synthesis gas and flue gas mixtures.

It should be noted here that the MOFs with coordinatively unsaturated metal centers have been anticipated to show high H_2 adsorption because H_2 adsorption is regarded as a mixture of physisorption and chemisorption. However, the present result indicates that coordinatively unsaturated metal centers in the MOF do not help the H_2 adsorption.

Sorption experiments with different solvents were carried out at 298 K (Figure 7b). It shows stepwise sorption for water, some hydroxylic molecules, and benzene. For water vapor adsorption, an increase in the amount of adsorbed vapor under low pressure ($0 < P/P_0 < 0.3$) indicates initial adsorption with one molecule of water per unit pore, and then at $0.3 < P/P_0 < 0.4$, a rapid increase of adsorption with two molecules of water per unit pore, and the third stepwise sorption at $0.4 < P/P_0 < 1.0$ is an adsorption with four molecules of water per unit pore. It was found that the desorption curve did not trace the

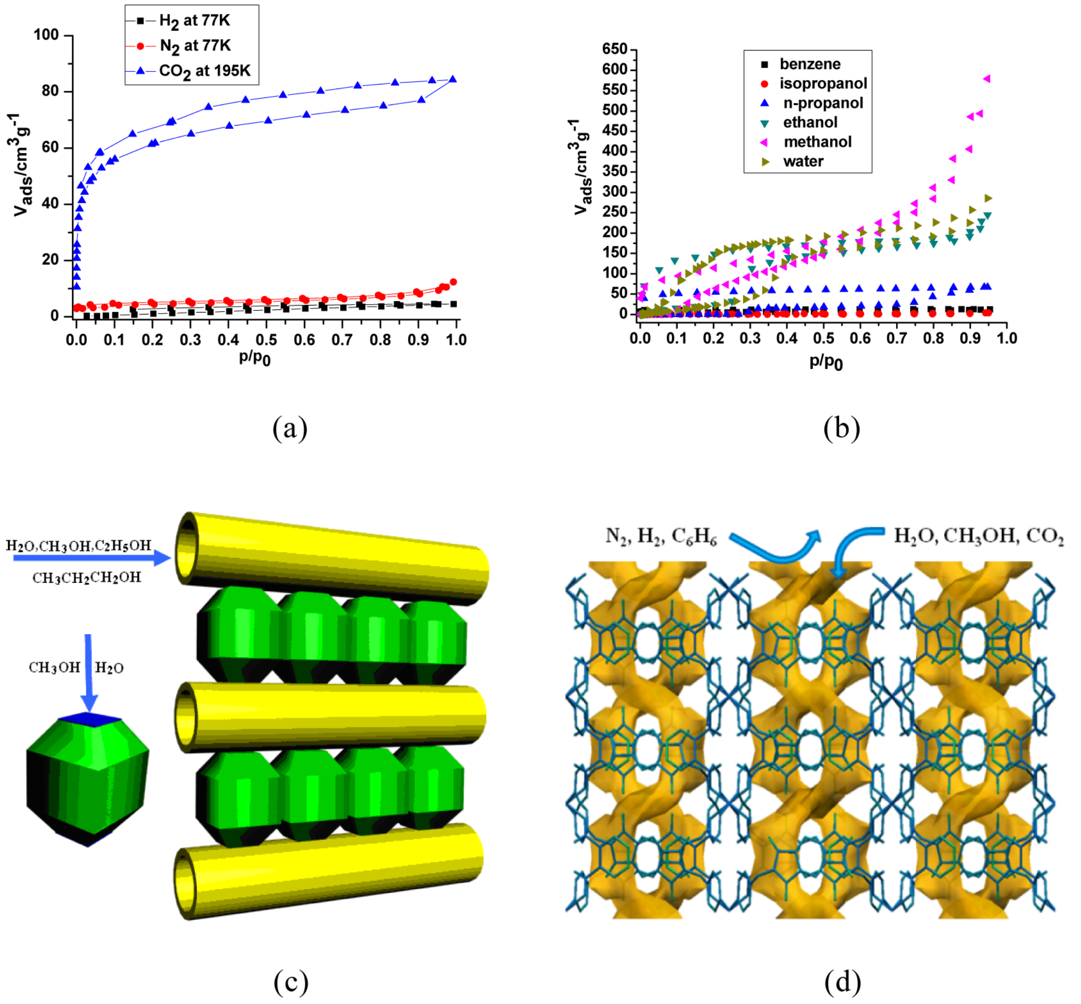

(a) (b)

(c) (d)

Figure 7. (a) Gas CO_2 at 195 K and H_2 and N_2 at 77 K adsorption/desorption isotherms for **2** after activation at 110 °C for 24 h. (b) H_2O, MeOH, EtOH, *n*-propanol, 2-propanol, and benzene vapor adsorption/desorption isotherms at 298 K for **2** after degassing for 24 h at 110 °C. (c) Schematic representation of the vapor adsorption. (d) Schematic representation of the selective adsorption.

adsorption curve any longer, which has a large hysteresis. According to the interesting phenomenon, we deduced that one water molecule is first adsorbed in the coordinatively unsaturated Cu^{2+} metal sites, the following two molecules of water enter the tetragonal cages in which one of the two water molecules is coordinated with unsaturated Cu^{2+} metal site, and finally, four molecules of water are adsorbed in the channels. The water molecules strongly interact with the Cu^{2+} metal sites and channels' surfaces, respectively, and therefore, desorption becomes difficult and shows a hysteresis profile. The above assumption is consistent with the results of single crystal X-ray diffraction analysis, which indicates that **2** could adsorb two water molecules at the unsaturated Cu^{2+} metal site in the framework. Similarly, the methanol (kinetic diameter = 3.6 Å) vapor adsorption curve shows that after an initial adsorption of about two molecules of methanol at $0.3 < P/P_0$ per unit pore, the adsorption of the other eight molecules of methanol occurred at $0.3 < P/P_0 < 1.0$. In the case of MeOH, two methanol molecules could be first adsorbed in the unsaturated Cu^{2+} metal sites and the following molecules of methanol are adsorbed in channels' surface by H-bonding interactions with the carbonyl groups of the ligand, which results in a two-step adsorption profile. The stepwise sorption curves of **2** for water and methanol show a hysteretic sorption behavior correlating with the diversity of the binding sites. On the other hand, at 298 K, ethanol (4.5 Å) can interact with the channels' surfaces and diffuse into the channels of **2**. However, ethanol molecules cannot enter the tetragonal cages because they are too large and thus cannot coordinate with the Cu^{2+} metal sites, as demonstrated by complex **2** not showing any color change when immersed in ethanol or ethanol vapor. The amount of adsorption was calculated using the Dubinin–Radushkevich equation, which shows that for every Cu^{2+} atom 7.0 water molecules, 11 methanol molecules, and 5 ethanol molecules can be absorbed into the microspores. Importantly, the *n*-propanol (4.7 Å) also can be adsorbed in **2**, and two-step adsorption profiles were observed. The amounts of *n*-propanol adsorbed corresponded to 1.5 molecules per formula, and we deduced that the *n*-propanol molecules are not allowed to enter the tetragonal cages owing to them, like ethanol, being too large (Figure 7c). The most interesting feature is that **2** takes up a much larger amount of *n*-propanol than 2-propanol molecules (4.7 Å) due to the effect of shape exclusion, indicating that **2** is a promising microporous material for the *n*-propanol/2-propanol separation at ambient temperature (Figure S3, Supporting Information). Moreover, the absorption experiments with benzene (5.3 Å) at 298 K show that benzene molecules cannot enter the channels of **2**. The selective sorption of water, methanol, and ethanol over benzene in **2** is due to selective H-bonds with the hydrophilic channels' surface, which helps alcohol solvents to enter the channels and small tetragonal cages (Figure 7d).

CONCLUSION

In summary, we have prepared a 3D open MOF **1** by using a flexible ligand and a second functional building unit from the simple solvothermal reaction. Although **1** has no free space because the methanol molecules coordinating Cu^{2+} ions and water molecules occupy the channels, they can be removed to obtain desolvated crystal **2**. Crystal **2**, containing accessible coordination sites on Cu^{2+} sites, reveals selective sorption capabilities for CO_2 gas and small hydroxylic molecules. The coordinatively unsaturated Cu^{2+} metal sites have strong interactions with some small hydroxylic molecules, and meanwhile, the other small hydroxylic molecules can be adsorbed in channels' surface by H-bonding interactions with the carbonyl groups of the ligand, which shows that the adsorbate−adsorbent interaction is very important in the selective sorption phenomenon. Furthermore, its adsorption capacity for CO_2 gas over N_2 and H_2 gases may be applied in the removal of CO_2 from synthesis gas and flue gas mixtures. The MOF selectively interacts with hydroxylic guests and shows sorption selectivity for water, methanol, ethanol, and *n*-propanol guests. Notably, this compound shows complete selectivity in adsorption for *n*-propanol over 2-propanol. Moreover, the coordinatively unsaturated Cu^{2+} centers selectively encapsulate hydroxylic guest molecules with the color changing in a reversible SC−SC fashion. This MOF is an important example of open hydrogen-bonding MOFs showing the ability for selective colorimetric detection of hydroxyl groups by the naked eye.

ASSOCIATED CONTENT

Supporting Information

Temperature-dependent XRPD patterns of complex **1**, TGA curves of complexes **1**−**3**, UV−vis spectra of purple **2** and blue **3** for four cycles, and sorption isotherms of **2** for *n*-propanol and 2-propanol molecules. This material is available free of charge via the Internet at http://pubs.acs.org.

AUTHOR INFORMATION

Corresponding Author

*Phone: +86-20-84115178. Fax: +86-20-84115178. E-mail: liujunm@mail.sysu.edu.cn; cesscy@mail.sysu.edu.cn.

Notes

The authors declare no competing financial interest.

ACKNOWLEDGMENTS

This work was supported by the 973 Program of China (2012CB821701), NSFC Projects (U0934003, 21173272, and 21121061), China Postdoctoral Science Foundation (20110490950, 2012T50737), Fundamental Research Funds for the Central Universities, and Technology Planning Project of Guangdong Province (2011J2200053).

REFERENCES

(1) (a) Moulton, B.; Zaworotko, M. J. *Chem. Rev.* **2001**, *101*, 1629. (b) Evans, O. R.; Lin, W. B. *Acc. Chem. Res.* **2002**, *35*, 511. (c) Caulder, D. L.; Raymond, K. N. *Acc. Chem. Res.* **1999**, *32*, 975. (d) Morgan, M.; Rebek, J. *Chem. Rev.* **1997**, *97*, 1647. (e) Kil, S. M.; Myunghyun, P. S. *J. Am. Chem. Soc.* **2000**, *122*, 6834. (f) Fujita, M.; Oka, H.; Yamaguchi, K.; Ogura, K. *Nature* **1995**, *378*, 469. (g) Chen, C. L.; Kang, B. S.; Su, C. Y. *Aust. J. Chem.* **2006**, *59*, 3. (h) Robin, A. Y.; Fromm, K. M. *Coord. Chem. Rev.* **2006**, *250*, 2127. (i) Nouar, F.; Eubank, J. F.; Bousquet, T.; Wojtas, L.; Zaworotko, M. J.; Eddaoudi, M. J. *J. Am. Chem. Soc.* **2008**, *130*, 1833.

(2) (a) Chen, B. L.; Ma, S. Q.; Hurtado, E. J.; Lobkovsky, E. B.; Zhou, H. C. *Inorg. Chem.* **2007**, *46*, 8490. (b) Ma, S. Q.; Wang, X. S.; Manis, E. S.; Collier, C. D.; Zhou, H. C. *Inorg. Chem.* **2007**, *46*, 3432. (c) Ghosh, S. K.; Zhang, J. P.; Kitagawa, S. *Angew. Chem., Int. Ed.* **2007**, *46*, 7965. (d) Tanaka, D.; Nakagawa, K.; Higuchi, M.; Horike, S.; Kubota, Y.; Kobayashi, T. C.; Takata, M.; Kitagawa, S. *Angew. Chem., Int. Ed.* **2008**, *47*, 3914. (e) Zhang, J. P.; Chen, X. M. *J. Am. Chem. Soc.* **2008**, *130*, 6010. (f) Wei, Y. L.; Hou, H. W.; Fan, Y. T.; Zhu, Y. *Eur. J. Inorg. Chem.* **2004**, *19*, 3946. (g) Ferey, G.; Mellot-Draznieks, C.; Serre, C.; Millange, F. *Acc. Chem. Res.* **2005**, *38*, 217. (h) Bradshaw, D.; Claridge, J. B.; Cussen, E. J.; Prior, T. J.; Rosseinsky, M. *Acc. Chem. Res.* **2005**, *38*, 273. (i) Rao, C. N. R.; Natarajan, S.; Vaidhyanathan, R. *Angew. Chem., Int. Ed.* **2004**, *43*, 1466. (j) Uemura, T.; Kitaura, R.; Ohta, Y.; Nagaoka, M.; Kitagawa, S. *Angew. Chem., Int. Ed.* **2006**, *45*, 4112. (k) Lee, J. Y.; Farha, O. K.; Roberts, J.; Scheidt, K. A.; Nguyen, S. T.; Hupp, J. T. *Chem. Soc. Rev.* **2009**, *38*, 1450.

(3) (a) Farha, O. K.; Spokoyny, A. M.; Mulfort, K. L.; Hawthorne, M. F.; Mirkin, C. A.; Hupp, J. T. *J. Am. Chem. Soc.* **2007**, *129*, 12680. (b) Cavka, J. H.; Jakobsen, S.; Olsbye, U.; Guillou, N.; Lamberti, C.; Bordiga, S.; Lillerud, K. P. *J. Am. Chem. Soc.* **2008**, *130*, 13850. (c) Allendorf, M. D.; Bauer, C. A.; Bhakta, R. K.; Houk, R. J. T. *Chem. Soc. Rev.* **2009**, *38*, 1330. (d) Rocha, J.; Carlos, L. D.; Paz, F. A. A.; Ananias, D. *Chem. Soc. Rev.* **2011**, *40*, 926. (e) Mishra, A.; Wernsdorfer, W.; Abboud, K. A.; Christou, G. *J. Am. Chem. Soc.* **2004**, *126*, 15648. (f) Lee, S. Y.; Park, S.; Kim, H. J.; Jung, J. H.; Lee, S. S. *Inorg. Chem.* **2008**, *47*, 1913. (g) Li, Z.; Li, M.; Zhou, X. P.; Wu, T.; Li, D.; Ng, S. W. *Cryst. Growth Des.* **2007**, *7*, 1992. (h) Meng, X.; Song, Y.; Hou, H.; Han, H.; Xiao, B.; Fan, Y.; Zhu, Y. *Inorg. Chem.* **2004**, *43*, 3528. (i) Du, M.; Bu, X. H.; Guo, Y. M.; Liu, H.; Batten, S. R.; Ribas, J.; Mak, T. C. W. *Inorg. Chem.* **2002**, *41*, 4904. (j) Lan, A.; Li, K.; Wu, H.; Olson, D. H.; Emge, T. J.; Hong, W.; Ki, M.; Li, J. *Angew. Chem., Int. Ed.* **2009**, *121*, 2370.

(4) (a) Wang, Z.; Cohen, S. M. *Chem. Soc. Rev.* **2009**, *38*, 1315. (b) Gadzikwa, T.; Farha, O. K.; Mulfort, K. L.; Hupp, J. T.; Nguyen, S. T. *Chem. Commun.* **2009**, 3720. (c) Farha, O. K.; Malliakas, C. D.; Kanatzidis, M. G.; Hupp, J. T. *J. Am. Chem. Soc.* **2009**, *132*, 950. (d) He, H.; Yuan, D.; Ma, H.; Sun, D.; Zhang, G.; Zhou, H. C. *Inorg. Chem.* **2010**, *49*, 7605. (e) Lun, D. J.; Waterhouse, G. I. N.; Telfer, S. G. *J. Am. Chem. Soc.* **2011**, *133*, 5806.

(5) (a) Li, K.; Olson, D. H.; Lee, J. Y.; Bi, W.; Wu, K.; Yuen, T.; Xu, Q.; Li, J. *Adv. Funct. Mater.* **2008**, *18*, 2205. (b) Férey, G.; Mellot-Draznieks, C.; Serre, C.; Millange, F. *Acc. Chem. Res.* **2005**, *38*, 217. (c) Kitaura, R.; Seki, K.; Akiyama, G.; Kitagawa, S. *Angew. Chem., Int. Ed.* **2003**, *42*, 428. (d) Hanson, K.; Calin, N.; Bugaris, D.; Scancella, M.; Sevov, S. C. *J. Am. Chem. Soc.* **2004**, *126*, 10502. (e) Dietzel, P. D. C.; Panella, B.; Hirscher, M.; Blom, R.; Fjellvåg, H. *Chem. Commun.* **2006**, 959. (f) Lee, E. Y.; Jang, S. Y.; Suh, M. P. *J. Am. Chem. Soc.* **2005**, *127*, 6374. (g) Beau-vais, L. G.; Shores, M. P.; Long, J. R. *J. Am. Chem. Soc.* **2000**, *122*, 2763. (h) Fang, Q. R.; Zhu, G. S.; Jin, Z.; Ji, Y. Y.; Ye, J. W.; Xue, M.; Yang, H.; Wang, Y.; Qiu, S. L. *Angew. Chem., Int. Ed.* **2007**, *46*, 6638.

(6) (a) Barbour, L. J. *Chem. Commun.* **2006**, 1163. (b) Murray, L. J.; Dincă, M.; Long, J. R. *Chem. Soc. Rev.* **2009**, 38, 1294. (c) Biradha, K.; Ramanan, A.; Vittal, J. J. *Cryst. Growth Des.* **2009**, *9*, 2969.

(7) (a) Caltagirone, C.; Gale, P. A. *Chem. Soc. Rev.* **2009**, *38*, 520. (b) Gale, P. A.; Garcıa-Garrido, S. E.; Garric, J. *Chem. Soc. Rev.* **2008**, *37*, 151.

(8) (a) Rawashdeh-Omary, M. A.; Rashdan, M. D.; Dharanipathi, S.; Elbjeirami, O.; Ramesh, P.; Rasika Dias, H. V. *Chem. Commun.* **2011**, 1160. (b) Jin, X. H.; Sun, J. K.; Cai, L. X.; Zhang, J. *Chem. Commun.* **2011**, 2667. (c) Tetilla, M. A.; Carla Aragoni, M.; Arca, M.; Caltagirone, C.; Bazzicalupi, C.; Bencini, A.; Garau, A.; Isaia, F.; Laguna, A. *Chem. Commun.* **2011**, 3805.

(9) Zhao, D.; Timmons, D. J.; Yuan, D.; Zhou, H. C. *Acc. Chem. Res.* **2011**, *44*, 123.

(10) (a) Lee, J.; Farha, O. K.; Roberts, J.; Scheidt, K. A.; Nguyen, S. T.; Hupp, J. T *Chem. Soc. Rev.* **2009**, *38*, 1450. (b) Corma, A.; Garc, H.; Xamena, F. X. L. *Chem. Rev.* **2010**, *110*, 4606. (c) Xiang, S.; Shi, J.; Zhang, J.; Global, J. *Inorg. Chem.* **2010**, *1*, 42.

(11) (a) Lu, X. Q.; Jiang, J. J.; zur Loye, H. C.; Kang, B. S.; Su, C. Y. *Inorg. Chem.* **2005**, *44*, 1810. (b) Lu, X. Q.; Jiang, J. J.; Zhang, L.; Chen, C. L.; Su, C. Y.; Kang, B. S. *Cryst. Growth Des.* **2005**, *5*, 419. (c) Su, C. Y.; Goforth, A. M.; Smith, M. D.; zur Loye, H. C. *Inorg. Chem.* **2003**, *42*, 5685.

(12) Sheldrick, G. M. *SHELX 97, Program for Crystal Structure Solution and Refinement*; Göttingen University: Göttingen, Germany, 1997.

(13) Chen, M. S.; Chen, M.; Takamizawa, S.; Okamura, T.; Fan, J.; Sun, W. Y. *Chem. Commun.* **2011**, 3787.

(14) Xamena, F. X. L.; Casanova, O.; Tailleur, R. G.; Garcia, H.; Corma, A. *J. Catal.* **2008**, *255*, 220.